HHS Public Access

Author manuscript

IEEE ASME Int Conf Adv Intell Mechatron. Author manuscript; available in PMC 2020 February 10.

Published in final edited form as:

IEEE ASME Int Conf Adv Intell Mechatron. 2018 July ; 2018: 21–27. doi:10.1109/aim.2018.8452704.

Direction of Slip Detection for Adaptive Grasp Force Control with a Dexterous Robotic Hand

Moaed A. Abd,
Department of Ocean & Mechanical Engineering, Florida Atlantic University, Boca Raton, FL 33431, USA

Iker J. Gonzalez,
Department of Computer & Electrical Engineering & Computer Science, Florida Atlantic University, Boca Raton, FL 33431, USA

Thomas C. Colestock,
Department of Ocean & Mechanical Engineering, Florida Atlantic University, Boca Raton, FL 33431, USA

Benjamin A. Kent,
Department of Mechanical Engineering, University of Akron, Akron, OH 44325, USA

Dr. Erik D. Engeberg
Department of Ocean & Mechanical Engineering, Florida Atlantic University, Boca Raton, FL 33431, USA

Abstract

A novel method of tactile communication among human-robot and robot-robot collaborative teams is developed for the purpose of adaptive grasp control of dexterous robotic hands. Neural networks are applied to the problem of classifying the direction objects slide against different tactile fingertip sensors in real-time. This ability to classify the direction that an object slides in a dexterous robotic hand was used for adaptive grasp synergy control to afford context dependent robotic reflexes in response to the direction of grasped object slip. Case studies with robot-robot and human-robot collaborative teams successfully demonstrated the feasibility; when object slip in the direction of gravity (towards the ground) was detected, the dexterous hand increased the grasp force to prevent dropping the object. When a human or robot applied an upward force to cause the grasped object to slip upward, the dexterous hand was programmed to release the object into the hand of the other team member. This method of adaptive grasp control using direction of slip detection can improve the efficiency of human-robot and robot-robot teams.

I. Introduction

Shortly after the advent of the artificial robotic hand, preventing grasped objects from being inadvertently dropped has been a priority [1]. This is a very important problem in the area of prosthetic hands, as limb-absent people do not have a direct sense of the grasp force applied

mabd2015@fau.edu.

by their artificial hands after amputation [2], [3], [4], [5]. The lack of haptic feedback can lead to frustrating situations where the grasped object is dropped or crushed due to a dearth of tactile information during typical object manipulation tasks [6].

This need has motivated the design of specialized sensors to detect when grasped objects are slipping [7], [8], [9]. The BioTac has recently emerged as a cutting edge multimodal tactile sensor to observe the state of robotic fingertips [10], [11]. The BioTac is a soft fluid-filled sensor; when the internal conductive fluid is deformed, the resultant fluid distribution affects the internal electrodes' impedances to indicate the force distribution on the fingertip surface.

Most of the prior efforts to detect whether a grasped object is slipping have used a combination of a specialized sensor and a signal processing algorithm; the frequency spectrum has been a popular indicator of slip where high frequency signal components are indicative of vibrations that occur when grasped objects slip [12].

In contrast, one novel aspect of this research is to detect the direction that a grasped object is slipping. Two different dexterous robotic Shadow Hands [13] were used in this paper which have been outfitted with two different BioTac sensors (Fig. 1). It is interesting to note that human grasp reflexes show different responses with respect to the direction that a grasped object slips, where more dangerous directions of slip are compensated for more aggressively [14].

The first goal of the present study is to derive a means of reliably detecting the direction of slip (DoS), which has been studied previously with a specialized sensor [15]. In contrast, artificial neural networks (ANNs) [16], [17], [18], [19] will be used in this study for real-time detection of the direction that objects slip relative to a Dexterous Shadow Hand using a BioTac sensor. Initially, experiments were conducted to induce slip with two different BioTac sensors, mounted to the first finger of two different Shadow Hands (Fig. 1). After successfully training the ANN classifiers to detect the direction of sliding motion, they were used as a low-level input to a top level robotic hand reflex, which is a novel embodiment of tactile perception for robotic action. The second goal of this study is to investigate the utility of the slip direction detection for robotic reflex development. To that end, case studies during a collaborative task of transferring a cup between two robots and from a robot to a human were performed. Specifically, downward slip prompted a grasp force increase to prevent dropping the object. Upward slip caused the Shadow Hand to open so that the other team member could take the cup.

The first novel contribution of this paper is the development of an ANN classifier to detect the direction a grasped object slips in a dexterous robotic hand. The second novel aspect of this paper is the use of slip direction detection for adaptive robotic grasp reflexes, which is a promising avenue in the future to improve the efficiency of human-robot and robot-robot teams.

II. METHODS

In this paper, an offline study was first conducted as a proof of concept for ANN classification. Then, an online study was performed to test the ANN classifier in real-time.

Finally, experiments were performed for adaptive robotic reflexes with human-robot and robot-robot teams. The large similarity of the hardware allowed for a transmittal of the offline techniques to be applied during the real-time experiment with only minor adjustments required.

A. Robot Hardware

1) Robotic Hardware for Offline Experiments: For the offline experiment, an anthropomorphic robotic C6M Shadow Hand (Shadow Robotics, London, UK) was used. The Shadow Hand possesses 20 actuated degrees of freedom (DOF) along with 4 underactuated joints for a total of 24 joints. The Shadow Hand was the end-effector of a 7 DOF Yaskawa Motoman SIA-10F arm Fig. 1(a).

The BioTac sensor from SynTouch was mounted onto the index fingertip. This BioTac incorporates 19 impedances measuring electrodes (taxels) spatially distributed as shown in Fig. 2(a). Among some of the benefits, the BioTac is able to detect forces, microvibrations, and temperature, this enabled us to determine the point of contact and accurately detect the direction of slip. Also, the BioTac SP offers an easy-mount integration for the Shadow Hand.

2) Robotic Hardware for Online Experiments:

The real-time classification experiments were conducted using a E2M3R Shadow Dexterous Hand, mounted to a 6 DOF UR-10 robotic arm (Universal Robots, Denmark), Fig. 1(b). The BioTac SP, with 24 taxels spatially distributed as shown in Fig. 2(b), was connected to the index fingertip and used for direction of slip detection in real-time experiments.

B. Offline Training Data Collection—Using Yaskawa's FS100 teaching pendant, a series of movement sequences of the Yaskawa SIA-10F arm were programmed to maneuver the Shadow Hand above a fixed glass surface, establish contact between the surface and the BioTac, and subsequently induce slip between the fingertip sensor and the surface in either the south (S) or west (W) directions Fig. 3(a). Initially, the Shadow Hand was positioned slightly above the surface, with an angle of $\pi/4$rad between the back of the palm and the surface. Each trial began with the Shadow Hand being lowered onto the surface by the arm at a rate of 10mm/s until contact was established. Once contact was established, the arm paused for a period of five seconds to allow the taxels to reach a steady state. Following this five second pause, the arm induced slip between the BioTac and the surface by moving linearly long the S or W directions for a further 10 seconds at one of two constant speeds (12.5mm/s or 25mm/s). Following this, the robotic arm came to rest and the trial was concluded.

Fifty total trials were conducted for each direction and speed of slip. In addition to varying the speed of slip for each direction, two separate coefficients of friction were evaluated. The above procedure was repeated on the same glass surface, but the surface was coated with a thin layer of vegetable oil to lower the coefficient of friction between the BioTac and the surface. In all, a total of 400 trials were conducted for this study 50 trials for each independent variable listed in TABLE I.

The taxel signals (e_1, …, e_{19}) were recorded with Robot Operating System (ROS). All taxel data were collected at 80Hz. Following data collection, the resulting raw signal data were manually annotated to mark the onset and cessation of slip during each trial. As the response of the BioTac at the onset of slip and immediately following was of primary interest, the resulting data sets were trimmed to include a 200ms window immediately prior to and following the onset of slip. These trimmed and annotated trials were subsequently used to train an ANN with the purpose of identifying the onset and direction of slip from the obtained tactile data.

C. Neural Network Training—Prior to training of the ANN, the resultant data were segmented using a time-based square windowing function. A window time (tw) was empirically chosen as 100ms. Using the taxel data contained within the window at step i, the input vector used to train the ANN was derived where the raw signal data for each taxel was concatenated into a single Rqx1 normalized vector x_{ADN}, where q is given as follows.

$$q = n_t * n_w \tag{1}$$

And

$$n_w = round(\frac{t_w}{t_s}) \tag{2}$$

where n_t is the number of taxels (electrodes) and n_w is the number of data samples in the window Fig. 4.

At each time step, the previous n_w samples from each electrode e_i are concatenated into a single vector x_{AD}. After concatenation, the resultant vector was normalized over the infinity norm. The normalized vector x_{ADN} is given by

$$x_{ADN} = \frac{1}{\|x_{AD}\|_\infty} x_{AD}, x_{AD} = \begin{bmatrix} \begin{bmatrix} e_1(1) \\ \vdots \\ e_1(n_w) \end{bmatrix} \\ \vdots \\ \begin{bmatrix} e_{19}(1) \\ \vdots \\ e_{19}(n_w) \end{bmatrix} \end{bmatrix} \tag{3}$$

While straightforward, the resulting dimension of the input layer of the ANN is dependent on the size of the window function tw and the sampling rate t_s.

1) Neural Network Architecture:

To classify slip characteristics from the obtained data, an ANN was constructed and trained using the MATLAB Neural Network Toolbox and the patternnet () function. A feedforward network structure with a single layer of hidden neurons was used. The activation function of

the hidden layer was chosen to be the Hyperbolic sigmoid transfer function, while the softmax () activation function was implemented for the output layer. All networks implemented supervised learning using backpropagation.

2) Classification Method for Offline ANNs:

Of interest in the current study is the ability of the ANN to classify one of four distinct output states: no slip (NS), incipient slip (IS), and the direction of slip (once gross slip occurs), denoted GS and GW to represent slip in the South and West directions, respectively (Fig. 3(a)). The resultant target matrix x_T is realized as:

$$x_T = \begin{bmatrix} NS & 0 & 0 & 0 \\ 0 & IS & 0 & 0 \\ 0 & 0 & GS & 0 \\ 0 & 0 & 0 & GW \end{bmatrix} \tag{4}$$

While assigning output classification targets for training, the classification target was defined as IS if the point at which slip was initiated fell within the time sample of the window function t_w. The training algorithm chosen was the Levenberg-Marquardt algorithm, defined as:

$$x_{(k+1)} = x_k - \left[J^T J + \mu I\right]^{-1} J^T e \tag{5}$$

In (5), J represents the Jacobian matrix of the first derivatives of the network errors with respect to the weights and biases, while e is a vector of network errors. μ is a scalar value that is decreased on each successful training step. The Levenberg-Marquardt algorithm is commonly used in pattern recognition and other applications [14], [15], [16], [17].

D. Datasets for Real-Time ANN Training—As will be subsequently shown in the results, the offline ANN classifier was highly successful in detecting the direction of slip; however, it was not capable of distinguishing between the two different friction coefficients or slip speeds. Thus, the real-time classification experiments largely focused on detecting the direction of slip in four different directions, North, South, East, and West Fig. 3(b)) with one coefficient of friction and one speed of slip.

Initially, the Shadow Hand was positioned slightly above the plexiglass and then lowered until the BioTac was in contact with the plexiglass. Once contact was established, the arm induced slip in one of the four directions analyzed in this study (Fig. 3(b)). After the period of slip was concluded, the hand was lifted off the surface to conclude the trial. Ten trials were conducted for each direction of slip as well as the touch (T) and no touch (NT) states, for a total of 60 trials. The output of the 24 taxels (e_1, …, e_{24}) of the BioTac SP were recorded using ROS. Similar to the offline experiment, following data collection, the resulting raw signal data from the taxels were manually annotated to mark the onset and cessation of slip during each trial. The signals were used to train an ANN to correctly classify the direction of slip from the obtained tactile data. BioTac SP surface contour plots

show the relative electrode impedances for the four different directions of slip along with the Touch and No Touch states (Fig. 5).

E. Real-Time ANN for Direction of Slip Detection—The signal processing and slip classification for the real-time experiments were performed in MATLAB/Simulink utilizing the pattern recognition toolbox. The toolbox was used to design and implement a feedforward neural network with a single hidden layer composed of ten hidden nodes. The neural network was designed to determine one of 6 potential classes: 4 slip direction classes (North, South, East, West) as well as Touch and No Touch states. First, the raw BioTac SP data was fed into Simulink from ROS via the Robotics Toolbox (Fig. 6). Once in the Simulink environment, the raw BioTac SP data were sent to the previously trained ANN for classification. Here, the direction of the slip was classified with the respective orientation (North, South, West, and East) or with the appropriate touch classification (Touch, No Touch). The resulting output was then processed and published back to the ROS environment.

F. Adaptive Grasp Synergy Control based on ANN Direction of Slip Detection

1) Robot-Robot Team Experiments:

After successfully identifying direction of slip in real-time, the same concept was applied to a scenario involving two collaborating robots: the Shadow Hand was used to grasp and transport a 3D printed cup within reach of a Baxter Robot (Rethink Robotics). Next, Baxter was programmed to grasp and lift the cup while the Shadow Hand was programmed to monitor the direction of slip detection from the BioTac SP sensor. When the ANN classifier detected the slip behavior from Baxter pulling up (Slip East), the Shadow Hand was programmed to open and release the object. This experiment was repeated ten times.

2) Human-Robot Team Experiments:

The same cup-transfer experiment was performed with a human in place of Baxter. When the Shadow Hand transferred the cup to the person, the human applied forces to the cup in different directions: downward (towards the floor) and upwards (away from gravity). In this situation, the Shadow Hand was programmed to tighten the grip force to prevent slip if the direction of slip was downward whereas the hand was programmed to open if the direction of slip was upward. This experiment was repeated ten times.

III. Results

A. Offline ANN Slip Classification

Fig. 7 shows example trials of the trimmed, raw taxel data ($\boldsymbol{e}_i$, i = 1, …, 19) obtained from the slip detection experiments with both speeds of slip (SoS), directions of slip (DoS), and coefficients of friction (CoF). For comparison purposes, each trial is plotted with respect to normalized time (with each trial representing approximately 15 seconds). The first spike in the taxel responses at the beginning of each trial represent deformation of the outer skin of the BioTac as it comes into contact with the surface. At $\boldsymbol{t}_n$ = 0:45 slip is induced via the robotic arm, producing a corresponding secondary spike in the taxel responses. The average classification accuracy is 91.40%. The overall classification accuracy in the IS condition is

lower than the remaining three conditions. It was also observed that no difference could be detected between the high and low slip speeds and friction coefficients.

B. Real-Time ANN Slip Direction Detection

Illustrative results for real-time classification for all ten testing trials for slipping (South and East) are presented in Fig. 8(a, b) respectively. It can be observed that there were minor differences in the classifier behavior across the trials in each direction, but the performance while sliding in any of the four directions of slip was highly successful with early 100% accuracy in each of the four directions.

Fig. 9 shows the photo sequence of one trial and the ANN classification output associated with the slip direction. As the hand was lowered, the no touch state was detected (Fig. 9(a)). When the hand initially contacted the surface, the touch state was detected (Fig. 9(b)). The arm then lowered the hand slightly farther to establish firm contact, causing the index finger to extend in the north direction, which is also reflected in the classifier output (Fig. 9(c)). Then, the arm caused the hand to slip in the south direction (Fig. 9(d, e)). Immediately after this, the hand was lifted off the surface, to return to the no touch state (Fig. 9(f)).

C. Adaptive Grasp Synergy Control using ANN Slip Direction Detection

1) Robot-Robot Experiments: Fig. 10 shows data corresponding to Fig. 11(a, b, c, d) which represents the photo sequence of the Shadow Hand passing the 3D printed cup to Baxter and subsequently, Baxter grabbing the object. As the Shadow Hand initiated the grasp closure onto the cup, motion was caused in the index finger abduction joint X4 (Fig. 3(c)), which produced a momentary state of East Slip classification (Fig. 10) before stably grasping the object. After the grasp closure was completed, the object was firmly grasped and the classifier detected the Touch class while the cup was transported toward Baxter. Once Baxter started to pull the object from Shadow Hand, the classifier successfully detected the Slip East class (upward, away from gravity) which prompted the Shadow Hand controller to release the object. All ten trials were completed successfully.

2) Human-Robot Experiments: Fig. 11(e, f, g, h) shows a photo sequence of a human interacting with the Shadow Hand. As shown in Fig. 11(f) a person was trying to press downward on the 3D printed cup to cause downward slip which caused the Shadow Hand robotic reflex to tighten the hand. Next, the person pulled up on the cup which cued the Shadow Hand to release the cup. Ten illustrative BioTac SP taxels during one trial (Fig. 12) show initially the steady state where the touch classification is detected. Then, at t = 12s, the person pressed down on the cup and the classifier detected slip West (towards the floor). Shortly afterwards, the person pulled upwards and the classifier detected slip East, prompting the Shadow and to open and release the cup. All ten trials were completed successfully in this manner. The increased accuracy for the online classifier (nearly 100%) compared to the offline classifier (91.4%) can be explained by the higher number of electrodes present in the BioTac SP. The additional 5 electrodes in the BioTac SP created a more descriptive feature vector allowing for increased classification accuracy.

IV. Conclusion

An ANN classifier was developed to detect the direction of sliding contact of objects grasped by robotic hands in real-time. The ANN was trained and evaluated with two different tactile sensors connected to two different robotic hands with high success rates. The ability to detect the direction of grasped object slip was used for adaptive grasp control in the context of both a human-robot and robot-robot collaborative task to pass a cup from the dexterous robotic hand to another robot or person. When downward slip was detected, the robotic hand tightened the grip force to prevent slip. When the person or robot applied an upward force to the cup, the dexterous robotic hand opened to release the cup into the possession of the other team member. This manner of adaptive robotic grasp reflex based on detection of the direction of object slip can be useful to improve the performance of human-robot and robot-robot teams working collaboratively.

Acknowledgments

This research was supported in part by NIH 1R01EB025819 and NSF awards 1317952, 1536136, and 1659484, and by I-SENSE at FAU

References

[1]. Salisbury L and Colman A,"A mechanical hand with automatic proportional control of prehension," Medical and Biological Engineering, vol. 5, pp. 505–511, 1967. [PubMed: 6056363]

[2]. Fougner A, Stavdahl O, Kyberd P, Losier Y, and Parker P," Control of upper limb prostheses: terminology and proportional myoelectric control - a review," IEEE Transactions on Neural Systems and Rehabilitation Engineering, pp. 663–677, 2012; DOI: 10.1109/TNSRE.2012.2196711. [PubMed: 22665514]

[3]. Kent B, Lavery J, and Engeberg E, Anthropomorphic Control of a Dexterous Artificial Hand via Task Dependent Temporally Synchronized Synergies, Journal of Bionic Engineering, vol. 11, p. 236–248, 2014, DOI: 10.1016/S1672-6529(14)60044-5

[4]. Kent B, Karnati N, and Engeberg E, Electromyogram Synergy Control of a Dexterous Artificial Hand, Journal of NeuroEngineering and Rehabilitation, vol. 11, 2014, DOI: 10.1186/1743-0003-11-41

[5]. Belter J, Segil J, Dollar A, and Weir R," Mechanical design and performance specifications of anthropomorphic prosthetic hands: a review," Journal of Rehabilitation, Research, and Development, vol. 50, pp. 599–618, 2013. [PubMed: 24013909]

[6]. Kent B and Engeberg E," Robotic Hand Acceleration Feedback to Synergistically Prevent Grasped Object Slip," IEEE Transactions on Robotics, vol. 33, pp. 492–499, 2017, DOI: 10.1109/TRO.2016.2633574.

[7]. Vatani M, Engeberg E, and Choi J," Force and slip detection with direct-write compliant tactile sensors using multi-walled carbon nanotubes/polymer composites," Sensors and Actuators A: Physical, vol. 195, pp. 90–97, 2013, DOI: 10.1016/j.sna.2013.03.019

[8]. Gunji D, Mizoguchi Y, Teshigawara S, Ming A, Namiki A, Ishikawaand M, et al.," Grasping force control of multi-fingered robot hand based on slip detection using tactile sensor," presented at the IEEE International Conference on Robotics and Automation, Pasadena, CA, USA, 2008.

[9]. Cranny A, Cotton D, Chappell P, Beeby S, and White N," Thickfilm force, slip and temperature sensors for a prosthetic hand," Measurement Science and Technology, vol. 16, pp. 931–941, 2005.

[10]. Fishel J and Loeb G," Bayesian exploration for intelligent dentification of textures," Frontiers in Neurorobotics, vol. 6, pp. 1–20, 2012. [PubMed: 22393319]

[11]. Wettels N, Parnandi A, Moon J, Loeb G, and Sukhatme G," Grip control using biomimetic tactile sensing systems," IEEE/ASME Transactions on Mechatronics, vol. 14, pp. 718–723, 2009.

[12]. Engeberg E and Meek S," Adaptive sliding mode control for prosthetic hands to simultaneously prevent slip and minimize deformation of grasped objects," IEEE/ASME Transactions on Mechatronics, vol. 18, pp. 376–385, 2013, DOI: 10.1109/TMECH.2011.2179061.

[13]. Kent B, Karnati N, and Engeberg E," Electromyogram synergy control of a dexterous artificial hand to unscrew and screw objects," Journal of NeuroEngineering and Rehabilitation, vol. 11, 2014, DOI: 10.1186/1743-0003-11-41.

[14]. Eliasson A, Forssberg H, Ikuta K, Apel I, Westling G, and Johansson R," Development of human precision grip v. anticipatory and triggered grip actions during sudden loading," Experimental Brain Research, vol. 106, pp. 425–433, 1995. [PubMed: 8983986]

[15]. Vatani M, Engeberg E, and Choi J," Detection of the position, direction and speed of sliding contact with a multi-layer compliant tactile sensor fabricated using direct-print technology," Smart Materials and Structures, vol. 23, 2014, 10.1088/0964-1726/23/9/095008

[16]. Demuth HB, Beale MH, De Jess O, and Hagan MT, Neural network design: Martin Hagan, 2014.

[17]. Zhao J, Xie Z, Jiang L, Cai H, Liu H, and Hirzinger G," Levenberg-Marquardt based neural network control for a five-fingered prosthetic hand," in Robotics and Automation, 2005. ICRA 2005. Proceedings of the 2005 IEEE International Conference on, 2005, pp. 4482–4487.

[18]. Zhang GP," Neural networks for classification: a survey," IEEE Transactions on Systems, Man, and Cybernetics, Part C (Applications and Reviews), vol. 30, pp. 451–462, 2000.

[19]. Ibn Ibrahimy M, Ahsan R, and Khalifa OO," Design and optimization of Levenberg-Marquardt based neural network classifier for EMG signals to identify hand motions," Measurement Science Review, vol. 13, pp. 142–151, 2013.

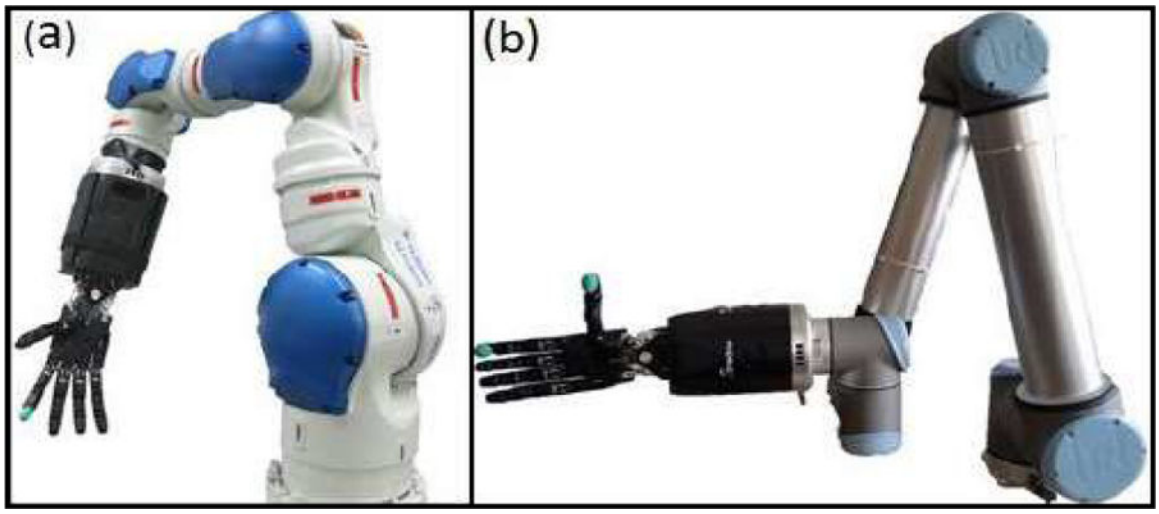

Fig. 1.
(a) Shadow hand mounted on Yaskawa Robotic Arm, (b) Shadow Hand Mounted on Universal Robot 10

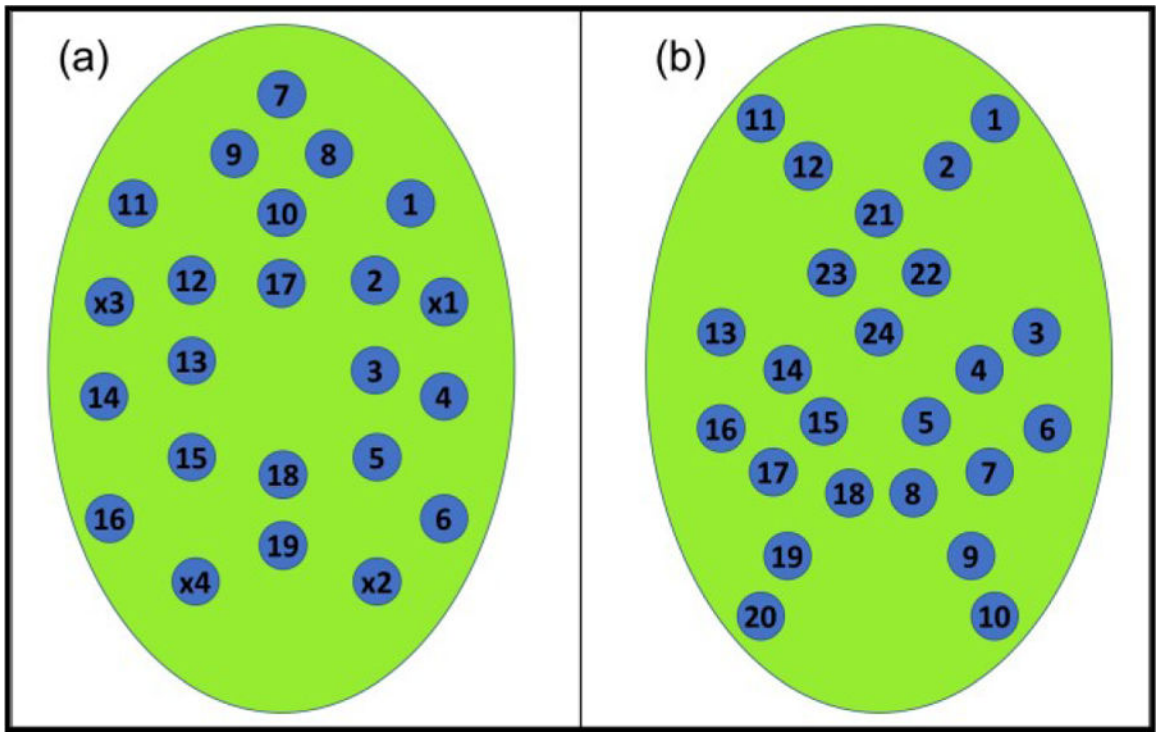

Fig. 2.

(a) Biotac Mapping representation of 19 electrodes. (b) Biotac SP Mapping representation of 24 electrodes

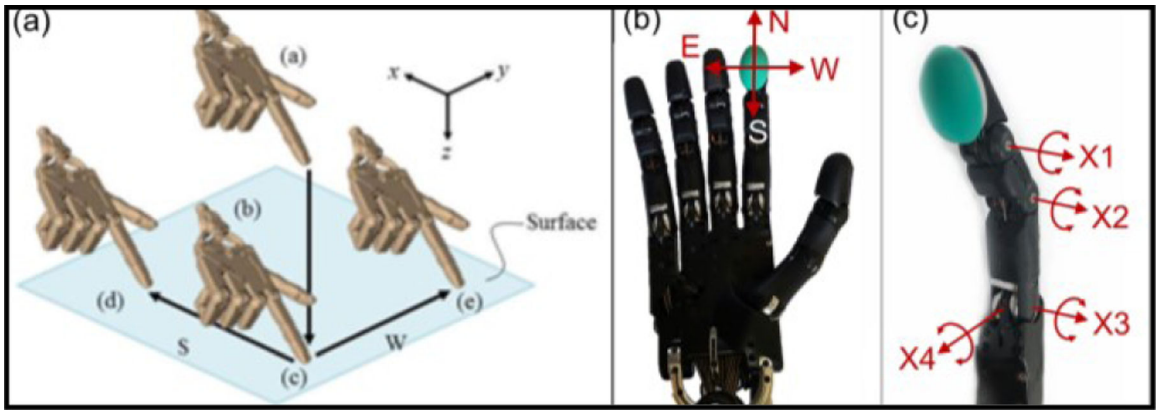

Fig. 3.

(a) Simulation of the performed slip detection experiments. (b) Direction representation for online experiment. (c) Joint angle labels for the index finger of the Shadow Hand.

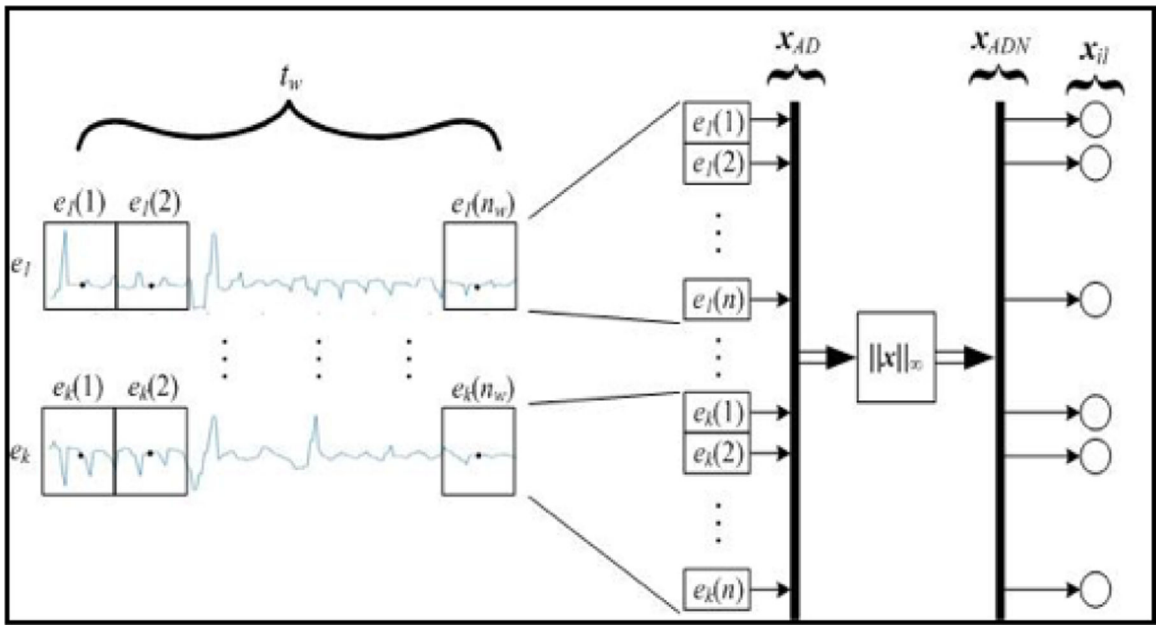

Fig. 4.

Block diagram representation of constructing the input vector using the AD Training approach.

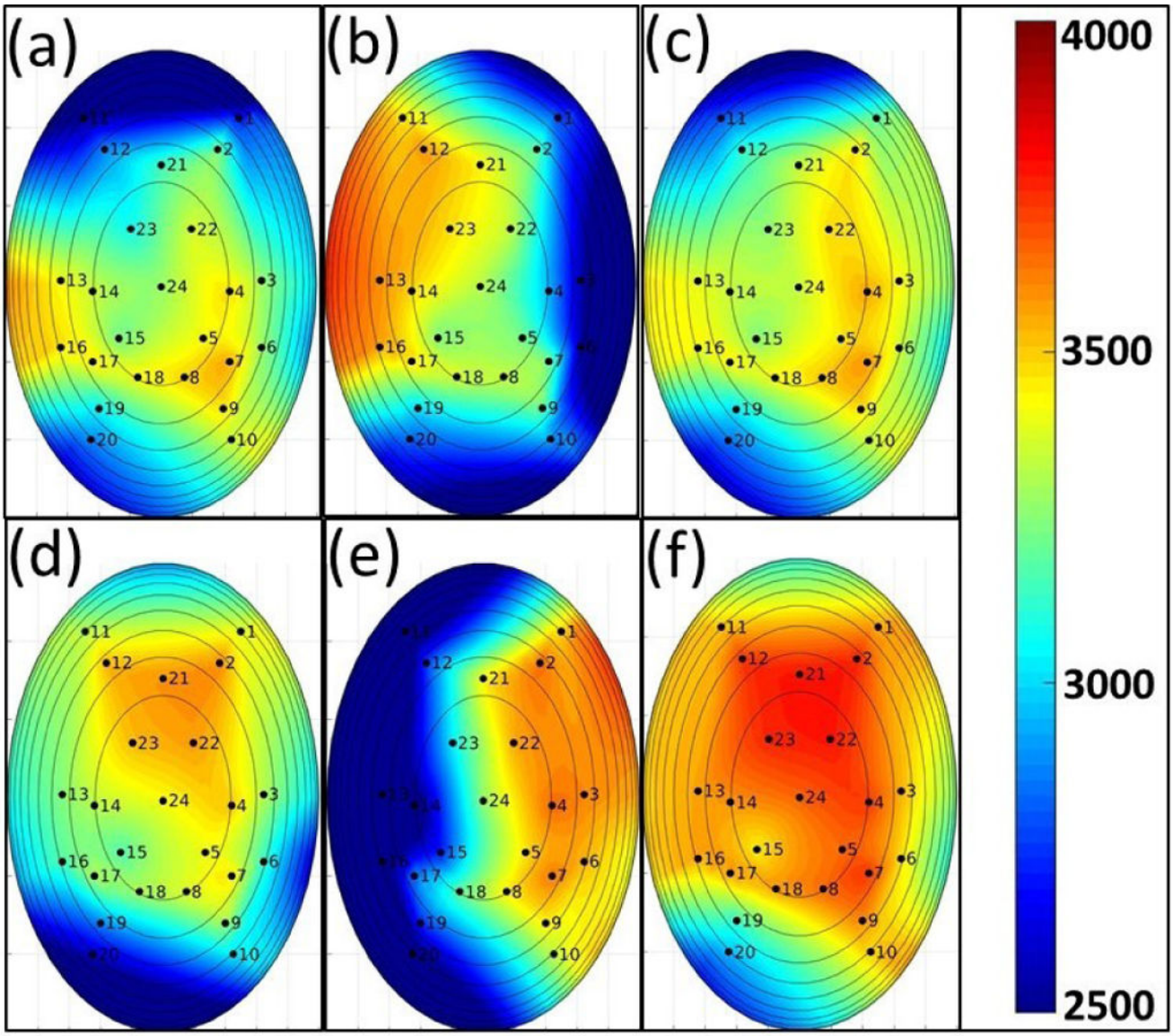

Fig. 5.

BioTac SP surface contours show the measured electrode impedances during the (a) Slip North (b) Slip East (c) Touch (d) Slip South (e) Slip West (f) No Touch trials.

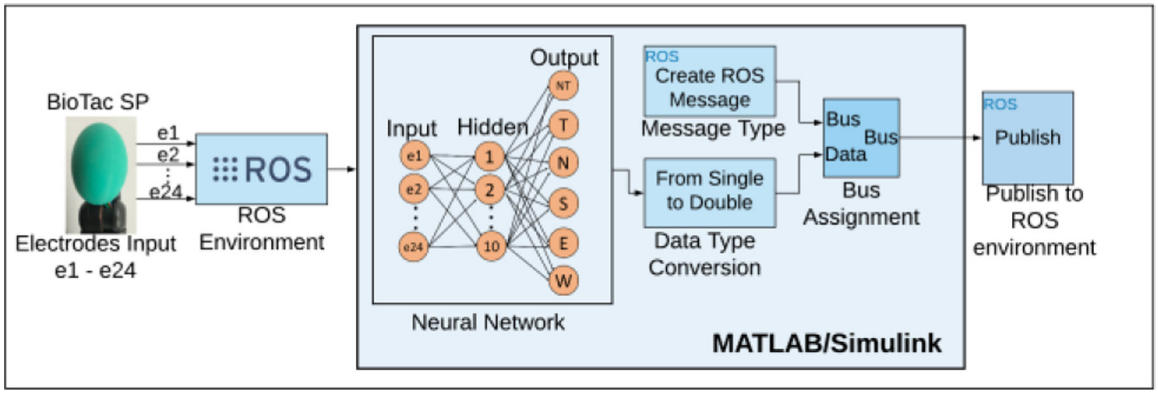

Fig. 6.

Classification flow architecture of online experiment, were the outputs of the Neural Network section correspond to the 6 classes NT (No Touch), T (Touch), N (North), S (South), E (East), W (West).

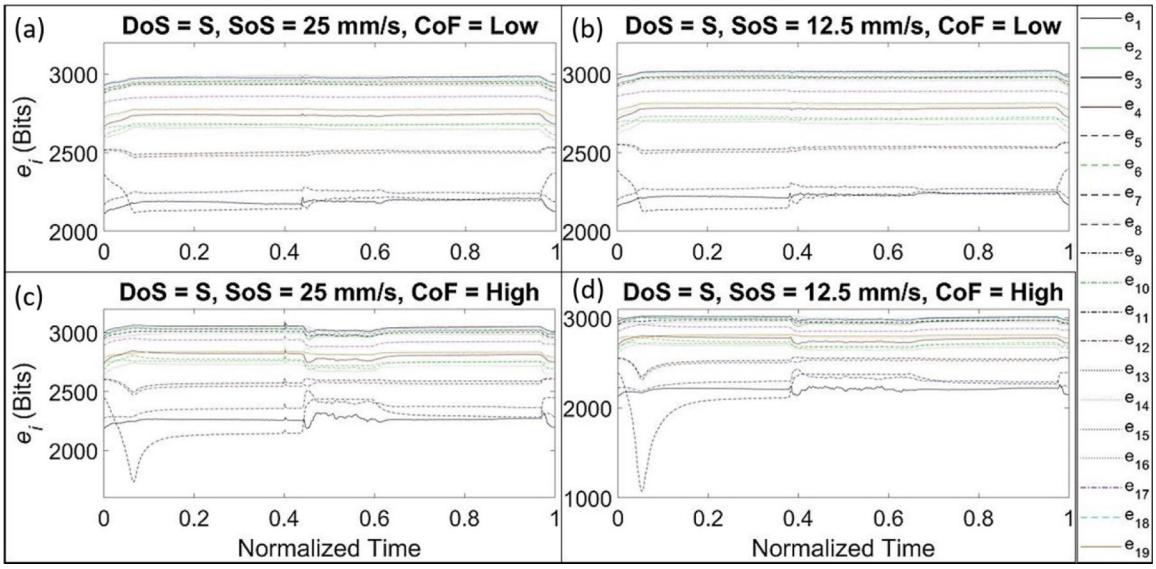

Fig. 7.

Example trials of Trimmed, raw taxel data for electrodes ($\boldsymbol{e}_1$, …, $\boldsymbol{e}_{19}$). (a) Taxel responses for DoS = S and CoF = Low (b) Taxel responses for DoS = S and CoF = Low. (c) Taxel responses for DoS = S and CoF = High (d) Taxel responses for DoS = S and CoF = High.

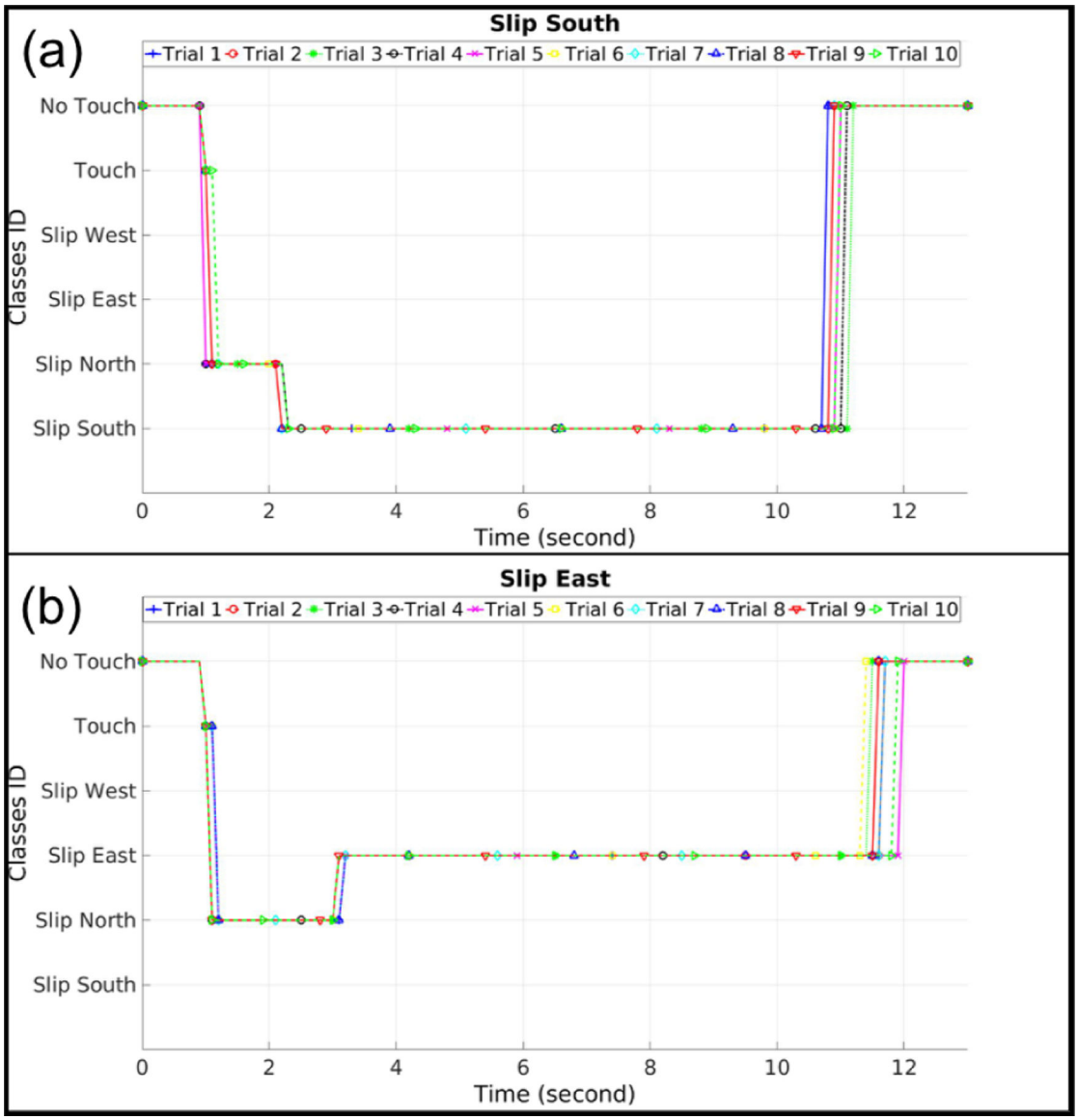

Fig. 8.

(a) Slip Classification results for all trials Slipping South, (b) Slip Classification results for all trials Slipping East

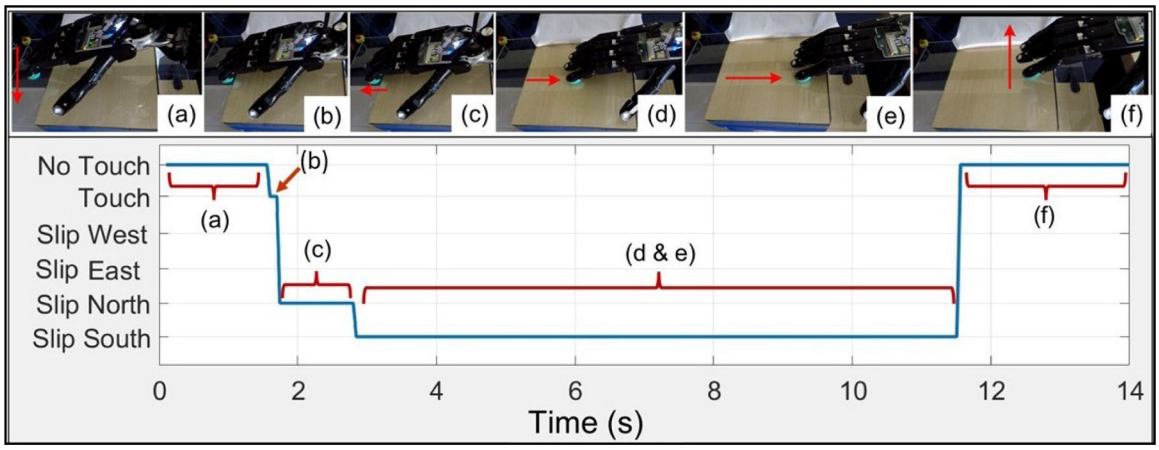

Fig. 9.

Photo sequence of Slip South scenario. (a) hand slightly above the glass. (b) Touch scenario (pre-slip). (c) Slip South starting point.

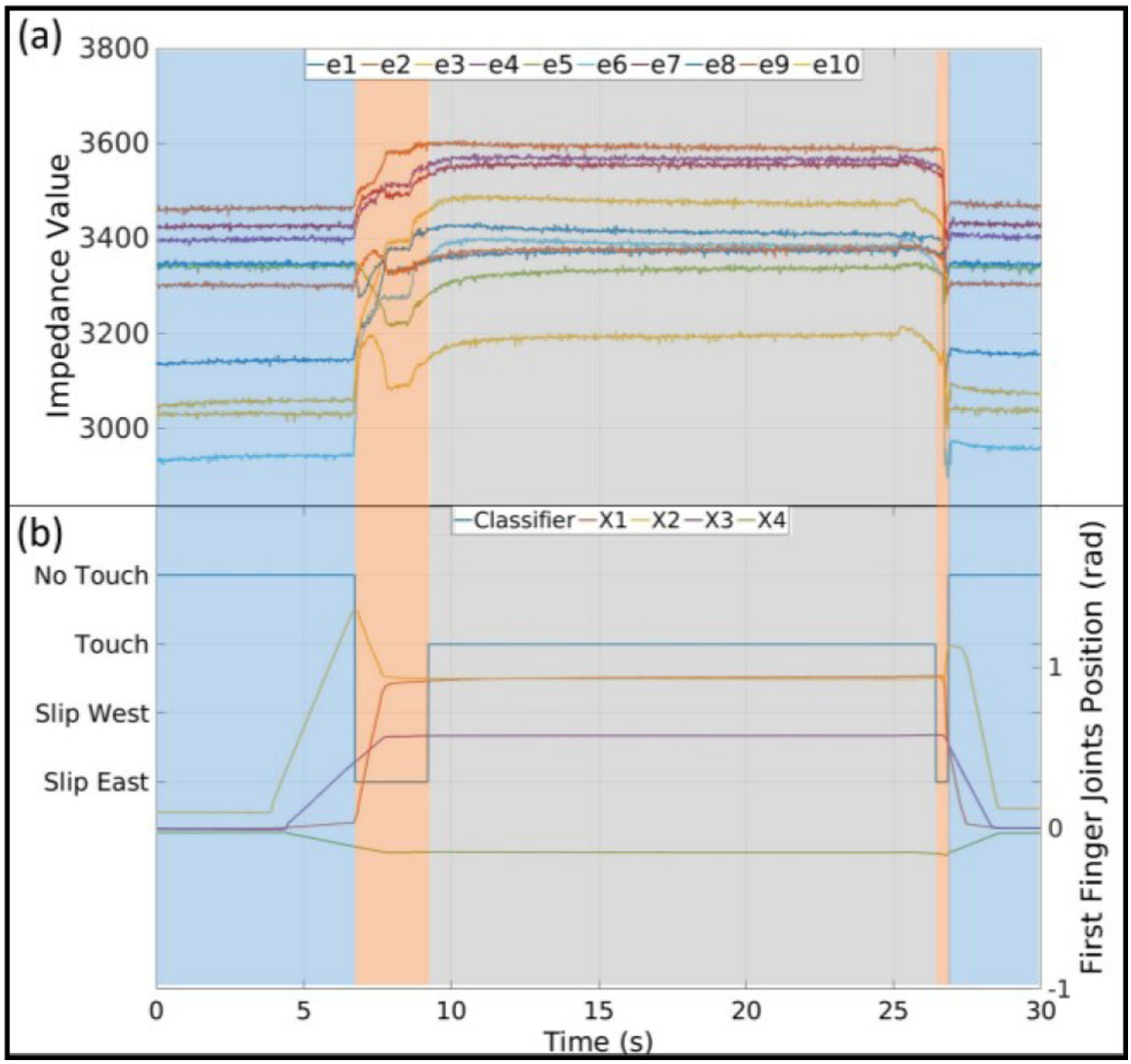

Fig. 10.

Robot-Robot Interaction Data corresponding to Fig. 11(a – d). (a) Electrodes Impedance for e1–e10, (b) Slip Classifier for Baxter-Shadow Interaction, and Shadow-Hand index finger joints position.

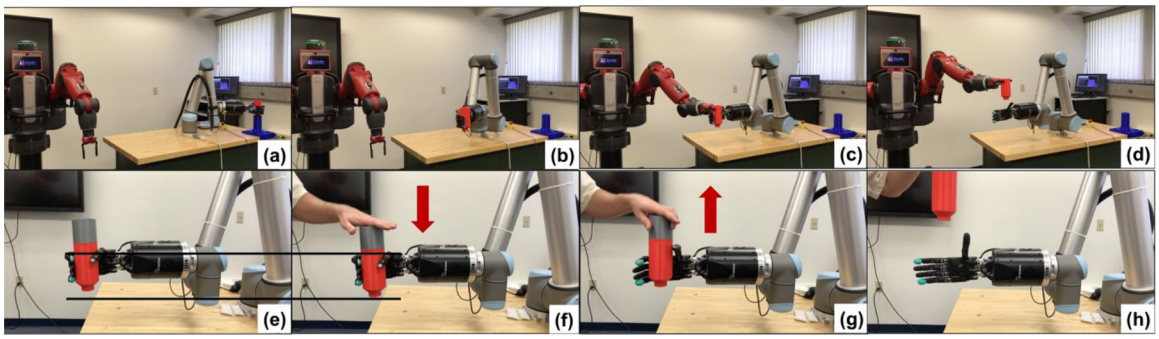

Fig. 11.

Robot-Robot interaction, (a, b, c, d) Photo sequence of Baxter Pulling Up the Cup from Shadow Hand. Human-Robot interaction (e, f, g, h) Photo sequence of Human Pushing Down and Pulling Up on the Cup from Shadow Hand.

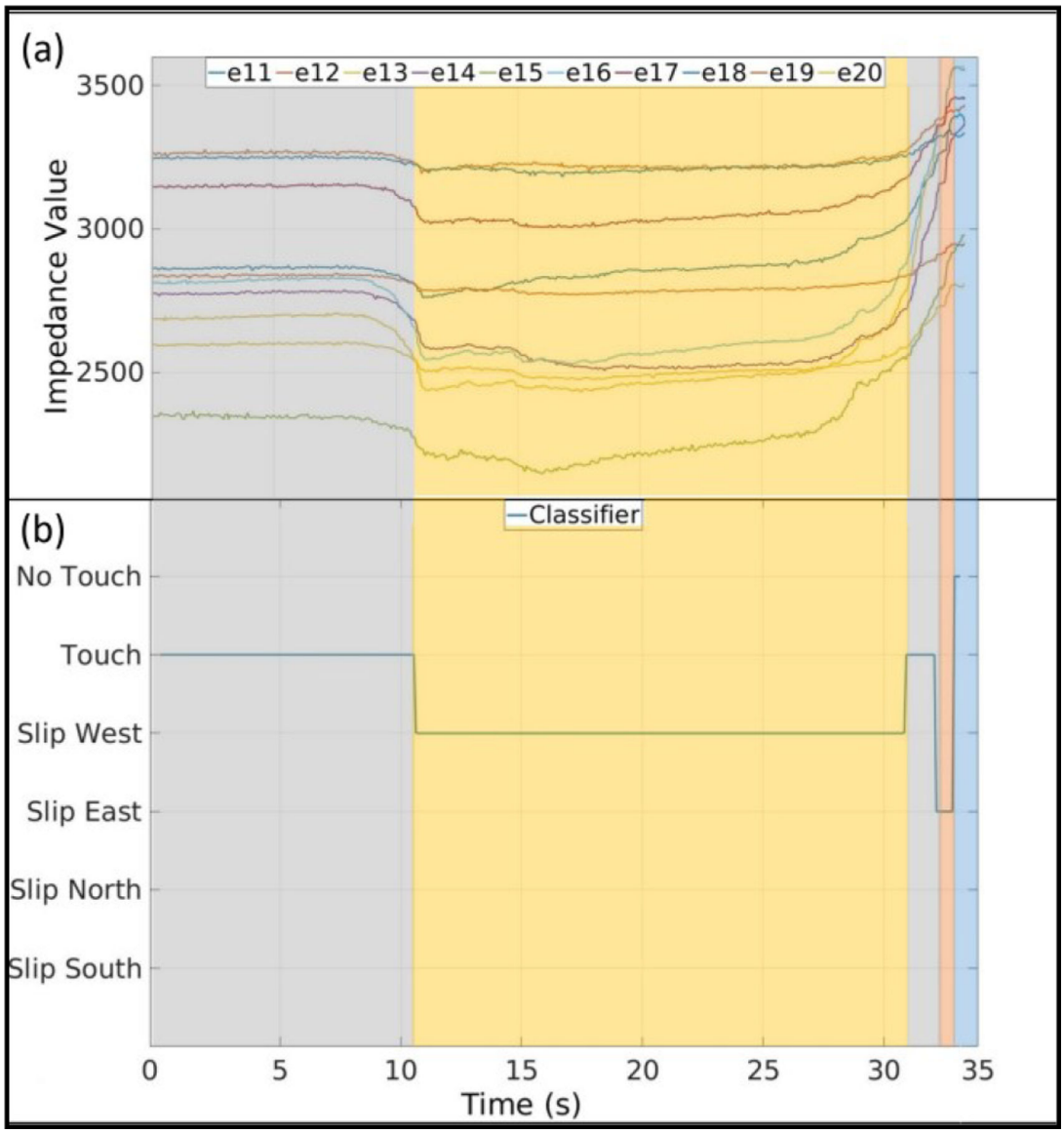

Fig. 12.

Human-Robot Interaction (a) Electrodes Impedance for e11–e20, (b) Slip Classifier for Human Robot interaction.

Author Manuscript

Author Manuscript

Author Manuscript

TABLE I

OFFLINE STUDY VARIABLES

Speed of Slip (SoS)	Direction of Slip (DoS)	Coefficient of Friction (CoF)
12.5/25 (mm/s)	South/West	High (Glass), Low (Glass with Oil)